

Crystal chemistry of silica-rich barium silicates

II: Electron microscopy of barium silicates containing multiple chains

Michael Czank* and Peter R. Buseck

Departments of Geology and Chemistry, Arizona State University,
Tempe, Arizona 85281, USA

Received: Oktober 9, 1978

Abstract. The phases containing multiple chains in the series $Ba_{m+1}[Si_{2m}O_{5m+1}]$ – those with triple ($m = 3$), quadruple ($m = 4$) and quintuple ($m = 5$) tetrahedral chains – were investigated by high resolution transmission electron microscopy. The resulting images could be correlated with the structures. Variations of the chain multiplicity (m) within single crystals were observed as well as faults in the packing of the multiple chains. The occurrence of sextuple ($m = 6$) chains suggests, that stable phases with $m > 5$ could also exist.

Introduction

A large number of silicates consist of strings of $[SiO_4]^{4-}$ tetrahedra linked by their corners to form chains, e.g., pyroxenes and amphiboles, or infinite sheets, e.g., micas, chlorites and clays. Until recently only chains of width one or two were known. An open question existed whether chains having widths greater than two occur naturally or could be made.

In the homologous series $Ba_{m+1}[Si_{2m}O_{5m+1}]$ it was found that the phases $Ba_4[Si_6O_{16}]$ ($m = 3$), $Ba_5[Si_8O_{21}]$ ($m = 4$) and $Ba_6[Si_{10}O_{26}]$ ($m = 5$) contain silicate chains of width 3, 4 and 5, respectively (all related references are given by Hesse and Liebau, 1980). These multiple chains are called triple, quadruple and quintuple chains, respectively, m being the multiplicity of the chains. The mineral sanbornite $Ba_2[Si_4O_{10}]$ and its high temperature form are sheet silicates and may be regarded as end members of this series with $m = \infty$. To date no ordered intermediates between $m = 5$ and $m = \infty$ have been reported.

* Permanent address: Mineralogisch-Petrographisches Institut der Universität Kiel, Olshausenstr. 40–60, D-2300 Kiel, Federal Republic of Germany

Recently, it was found that triple chains also occur in other silicates (Drits et al., 1974; Hutchison et al., 1975; Veblen and Burnham, 1978) as well as multiple chains of higher order (Veblen et al., 1977).

In the present study we have used high resolution transmission electron microscopy (HRTEM) to investigate the Ba chain silicates a) to see whether the chains could be imaged, b) to determine whether there are chains of different multiplicities within a single crystal, c) to assess the degree of disorder, d) to determine whether phases having chain multiplicities greater than five could occur, and e) to explore ways in which deviations from stoichiometry can be accommodated.

Structural considerations

The reported cell parameters and space groups of the barium chain silicates are given in Table 1. For $\text{Ba}_6[\text{Si}_{10}\text{O}_{26}]$ these are given for a primitive cell as well as for a B-centered cell and its corresponding transformation matrix. This B-centered cell is more convenient for interpreting the electron microscopic data and will therefore be used in the following discussion.

The multiple chains are oriented with their lengths parallel to [010] and their widths roughly parallel to [100]. Thus, the plane in which the multiple chains lie is almost parallel to (001) (Figs. 1a – c). The single tetrahedral chain outlined by heavier lines in the figures will be called a *subchain* so that, for example, there are five subchains in a quintuple chain (Fig. 1c).

Although all of the multiple chains in one structure are symmetrically identical, they assume differing orientations, most easily seen by reference to the [010] projections in Figures 1a – c. Within a multiple chain of $\text{Ba}_4[\text{Si}_6\text{O}_{16}]$ and $\text{Ba}_5[\text{Si}_8\text{O}_{21}]$ the tetrahedral apices pointing along the chain length are all

Table 1. Lattice constants (standard deviations are of the magnitude of the last columns)

Phase	<i>a</i> [Å]	<i>b</i> [Å]	<i>c</i> [Å]	β [°]	Space group
Conventional unit cells					
$\text{Ba}_4[\text{Si}_6\text{O}_{16}]$	12.477	4.685	13.944	93.54	$P2_1/c$
$\text{Ba}_5[\text{Si}_8\text{O}_{21}]$	32.675	4.695	13.894	98.10	$C2/c$
$\text{Ba}_6[\text{Si}_{10}\text{O}_{26}]$	20.196	4.707	13.842	98.61	$P2_1/c$
Centered unit cell					
$\text{Ba}_6[\text{Si}_{10}\text{O}_{26}]$	40.67	4.707	13.842	101.05	$B2_1/c$

$$\text{Transformation matrix} \begin{pmatrix} 2 & 0 & 1 \\ 0 & \bar{1} & 0 \\ 0 & 0 & \bar{1} \end{pmatrix}$$

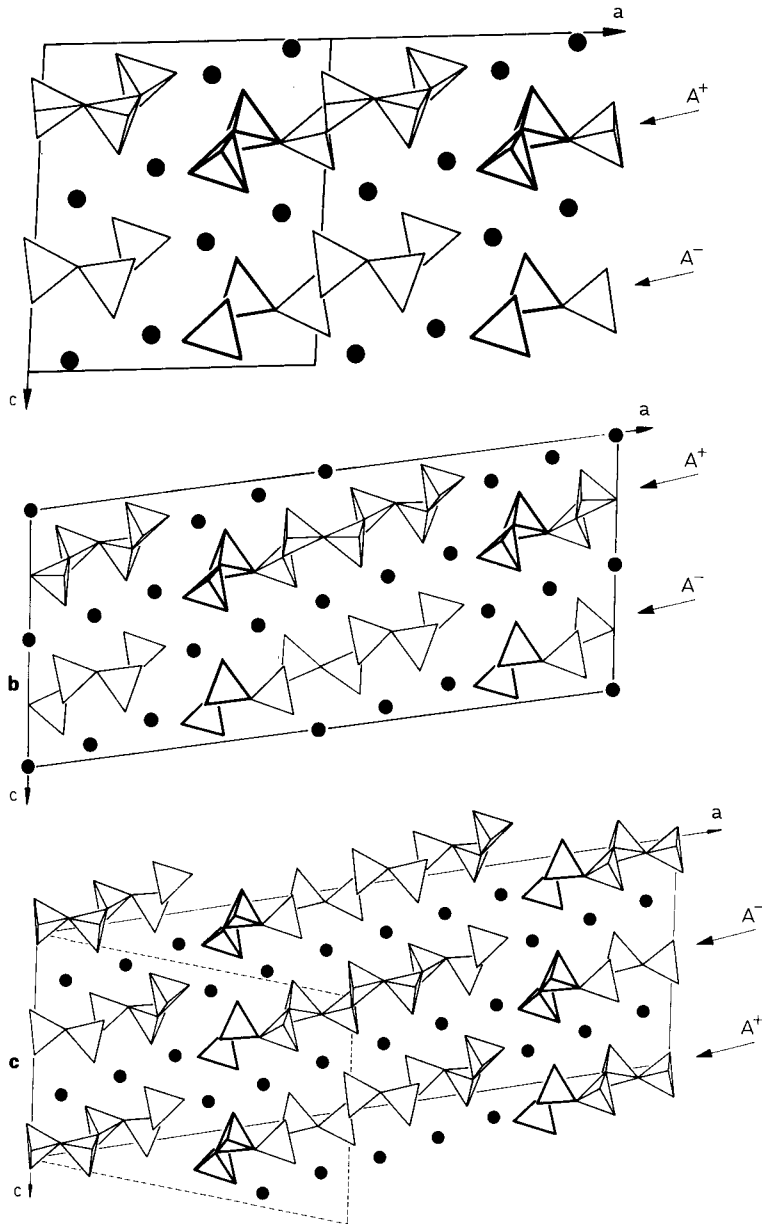


Fig. 1. Projection of the structure of the Ba silicates onto (010): a) $\text{Ba}_4[\text{Si}_6\text{O}_{16}]$, b) $\text{Ba}_5[\text{Si}_8\text{O}_{21}]$, c) $\text{Ba}_6[\text{Si}_{10}\text{O}_{26}]$. The length of the multiple chains is perpendicular to the plane of projection and their width is almost parallel to **a**. For illustration, one subchain of each multiple chain is outlined by heavy lines. The multiple chains have two orientations labelled A^+ and A^- ; they are joined by Ba atoms, indicated by black dots. In c) the dashed line indicates a primitive cell and the solid line a B-centered cell, the setting adopted in this paper

directed toward $+\mathbf{b}$ or all toward $-\mathbf{b}$. We will designate a multiple chain A^+ if the tetrahedral apices point toward $+\mathbf{b}$. Adjacent chains in the c direction are centrosymmetric to A^+ and have their tetrahedral apices in reverse orientation. These chains will be called A^- . In $\text{Ba}_6[\text{Si}_{10}\text{O}_{26}]$ quintuple chains alternating in the c direction will be designated A^+ and A^- in the same manner.

In order to understand the topological relations among the several compounds, one has to consider the arrangement of adjacent multiple chains in the $[100]$ direction (Figs. 2a–c). For structures having an even number of subchains, i.e. $\text{Ba}_5[\text{Si}_8\text{O}_{21}]$, the adjacent multiple chains are shifted by $\mathbf{b}/2$. This is a result of trying to obtain the best possible Ba–O polyhedron. Such a structure is C-centered rather than primitive, as in the case of structure with odd numbers of subchains.

Looking at the structures of these phases, pronounced cleavages would be expected parallel to the \mathbf{b} -axes (cf. Figs. 1 and 2). In fact, during electron microscopy most of the samples were observed as cleaved parallel to one of the planes (100), (001), or (102).

Experimental

For our investigations we used materials synthesized by H. Katscher and by R. Roth (Roth and Levin, 1959). The crystals from Katscher are from the same synthesizing run as the crystals used for X-ray studies (Hesse and Liebau, 1980). All phases were assumed to have the exact stoichiometric chemical compositions, although no analyses were made to confirm these compositions.

The samples for the high resolution electron microscope study were ground and deposited on a perforated carbon film. A modified Jeol JEM 100B electron microscope was used; sample preparation procedures and instrumental parameters were as described by Buseck and Iijima (1974).

Images discussed in the section on “Unperturbed Crystals” show the structure of the Ba silicates. These images were obtained at the conditions of critical alignment, underfocus, etc., as given by Buseck and Iijima (1974). In a subsequent paper, Iijima and Buseck (1978) showed that if structure images can be correlated with one dimensional lattice fringes, then it is reasonable to interpret the periodicities of the fringes in terms of the structure images. We use such fringes for many of our subsequent observations.

Observations

A large number of crystals of each composition were studied. No differences were noted between the specimens synthesized by Katscher and those by

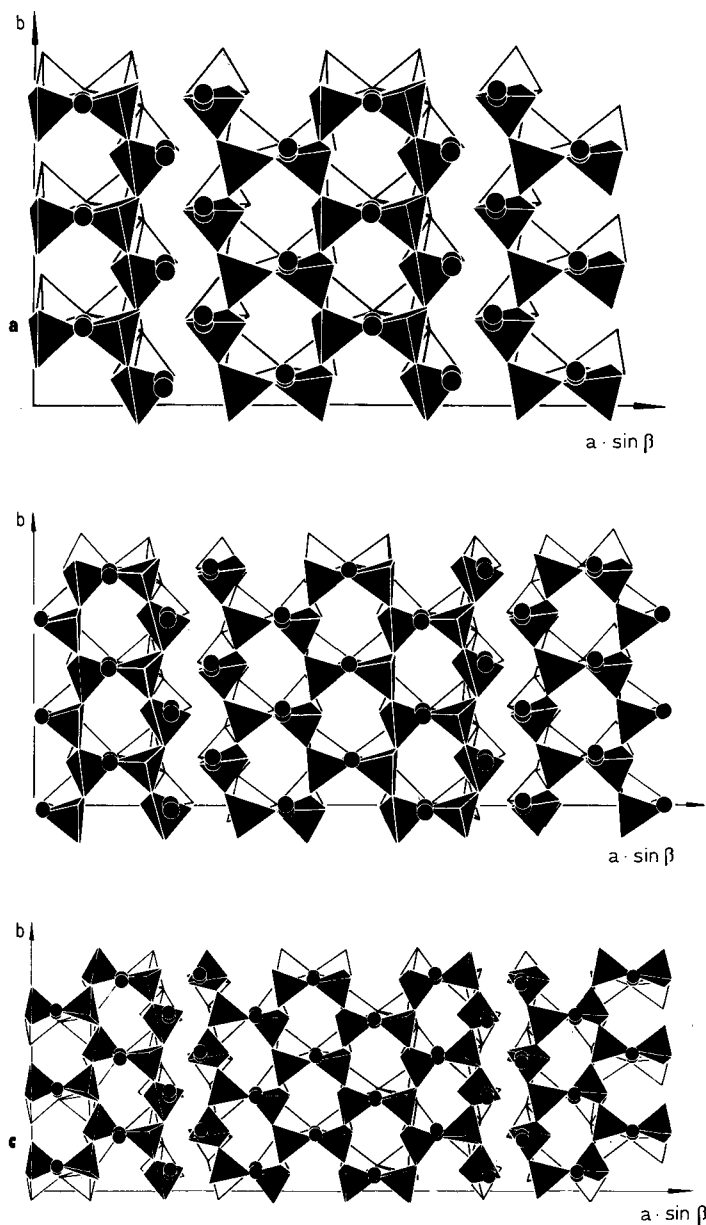


Fig. 2. Projections of the structures parallel to [001]: a) $Ba_4[Si_6O_{16}]$, b) $Ba_5[Si_8O_{21}]$, c) $Ba_6[Si_{10}O_{26}]$. In contrast to the others, in $Ba_5[Si_8O_{21}]$ the adjoining multiple chains in the [100] direction are shifted by $b/2$ relative to one another; this has the effect of producing a C-centered cell. The Ba atoms are positioned at the sides of interstices between the subchains, resulting in tunnels running through the structure. The anterior Ba atoms are positioned in front of the chains and the posterior Ba atoms between the chains

Roth. After grinding, most crystals are thin plates elongated parallel to **b**. They lie mainly on (100) for $\text{Ba}_4[\text{Si}_6\text{O}_{16}]$, and on (001) or (102) for $\text{Ba}_5[\text{Si}_8\text{O}_{21}]$ and $\text{Ba}_6[\text{Si}_{10}\text{O}_{26}]$. These preferred orientations are a result of the good cleavages mentioned above. Because of the good cleavage, no crystals were found in an orientation with **b** parallel to the electron beam, i.e., with the chains running parallel to the beam.

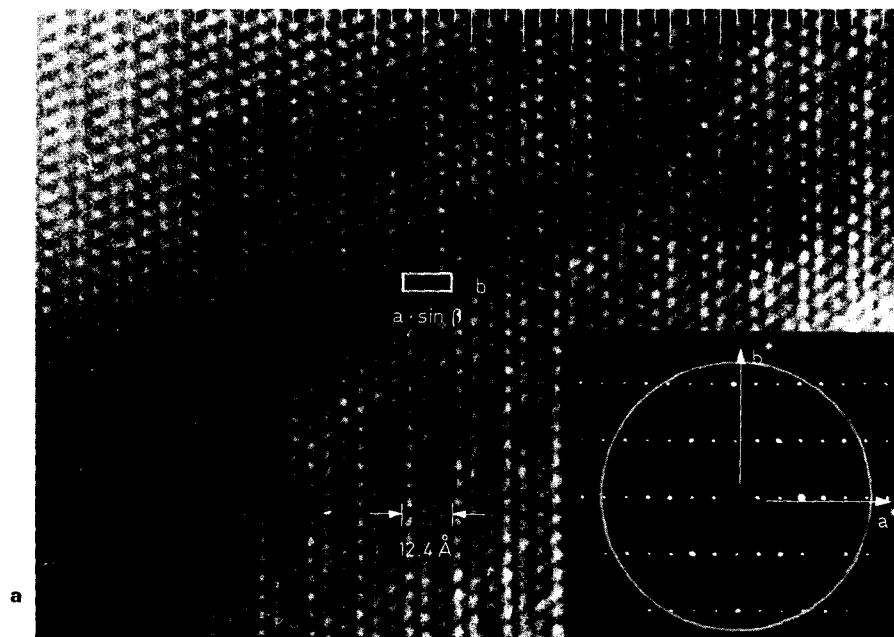
Although subjective, it appears as if $\text{Ba}_4[\text{Si}_6\text{O}_{16}]$ suffers less radiation damage than $\text{Ba}_5[\text{Si}_8\text{O}_{21}]$ or $\text{Ba}_6[\text{Si}_{10}\text{O}_{26}]$. It seems, subject to future confirmation, that the greater the similarity to a sheet structure, the greater the susceptibility to radiation damage.

Because of the fast radiation damage it was difficult to obtain through-focus series, which is essential for HRTEM work. The differences in focal conditions together with minor variations of thickness and orientation are presumably the reason for some considerable variations in the images in several figures.

We will first describe and discuss observations of crystals that approximate the ideal structures, followed by examples of disordered crystals.

Unperturbed crystals

The high resolution structure images shown in Figures 3a–c illustrate the chain configurations in $\text{Ba}_4[\text{Si}_6\text{O}_{16}]$, $\text{Ba}_5[\text{Si}_8\text{O}_{21}]$ and $\text{Ba}_6[\text{Si}_{10}\text{O}_{26}]$. They



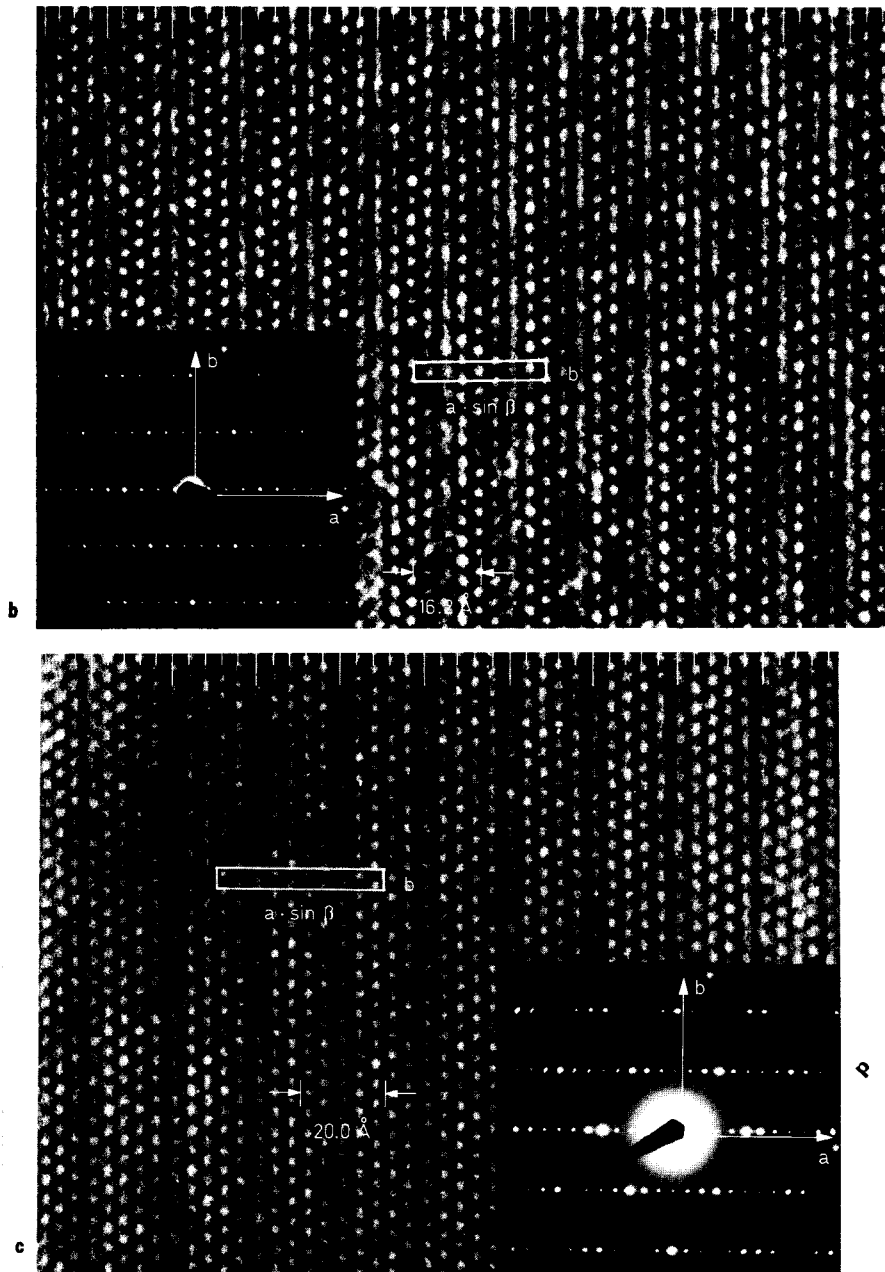


Fig. 3. High resolution images of a) $Ba_4[Si_6O_{16}]$, b) $Ba_5[Si_8O_{21}]$, c) $Ba_6[Si_{10}O_{26}]$ with their corresponding electron diffraction patterns. In a) the objective aperture is indicated by the white circle. Unit cells are marked by white boxes. The scales indicate the approximate widths of the multiple chains. For further discussion see text

were taken with [001] parallel to the electron beam. Corresponding electron diffraction patterns are shown in the insets, with the objective aperture indicated by the white circle in Figure 3a. The same aperture was used for the subsequent figures.

Prominent in the images are white spots having a periodicity of 4.7 Å parallel to \mathbf{b}^* . Note that in the case of the quintuple chains (Fig. 3c) there is a sequence of four of such rows of clearly recognizable spots perpendicular to \mathbf{b}^* (marked by short ticks on the upper edge of the figure), followed by a slightly streaked line of almost uniform brightness (marked by the longer ticks).

We interpret the spots as corresponding to the tunnels running parallel to [001] between the subchains (Fig. 2c). The streaked lines correspond to the planes parallel to (100) between adjacent chains. The darker contrast may be a consequence of the higher population of Ba atoms near this plane. In some areas this darker zone appears to be shifted slightly, presumably the result of minor misorientation of the crystal.

The images of crystals composed of triple and quadruple chains (Figs. 3a and b) show similar features to those of $\text{Ba}_6[\text{Si}_{10}\text{O}_{26}]$. In these cases, however, the rows of spots have a periodicity of two and three, respectively, perpendicular to \mathbf{b}^* . There is again an accordance between these spots and the tunnels (cf. Figs. 2a and b). We therefore assume that the pictures are the two dimensional structure images of these phases.

The apparent unit of periodicity in the [100] direction in the images of $\text{Ba}_4[\text{Si}_6\text{O}_{16}]$ and $\text{Ba}_6[\text{Si}_{10}\text{O}_{26}]$ correspond to the width of the triple and quintuple chains, respectively, as well as to the primitive cells (cf. Fig. 2a, c). In the case of $\text{Ba}_6[\text{Si}_{10}\text{O}_{26}]$, however, this periodicity is the half of the centered cell that was chosen in this paper. This is a consequence of the superposition of A^+ and A^- chains along [001] which precludes being able to distinguish between the two projected halves of the unit cell. Whereas in the image of $\text{Ba}_5[\text{Si}_8\text{O}_{21}]$ the unit of periodicity corresponds to the width of two quadruple chains and with that to the full dimension of the C-centered unit cell parallel to \mathbf{a}^* . This is a result of the relative shift in position of the chains by $\mathbf{b}/2$ (cf. Fig. 2b), apparent as an offset of spots in adjacent quadruple chains in this direction (Fig. 3b).

Perturbed crystals

There are several types of structural disorder which can occur in the Ba chain silicates. These have not been determined by X-ray studies, but can be studied by electron microscopy. We are interested in variations in chain multiplicities from the ideal value for a given compound and stacking faults in the sequences of chains.

Multiplicity faults

Recent electron microscopy of pyroxenes and amphiboles has shown that low concentrations of chains of differing width can occur within a material that is apparently homogeneous to X-ray diffraction and light optics (Buseck and Veblen, 1978). Similar deviations could be expected in the Ba silicates.

Variations in chain widths were recognized by observing and measuring the spacings between the one dimensional fringes parallel to (100). These spacings are 12.4 Å, 16.2 Å and 20.0 Å for triple, quadruple and quintuple chains, respectively. In crystals having the quadruple chain structure and, less frequently, in those having the quintuple chain structure we observed chains of other multiplicities; crystals having the triple chain structure, however, seemed uniform in chain width. Triple chains (Fig. 4a) and, less commonly, quintuple chains (Fig. 4b), occur as errors within the normal quadruple chain structure of $\text{Ba}_5[\text{Si}_8\text{O}_{21}]$. A few crystals have a sufficiently high concentration of triple chains to produce diffuse streaks perpendicular to \mathbf{b}^* on diffraction patterns with weak maxima at spacings corresponding to $\text{Ba}_4[\text{Si}_6\text{O}_{16}]$ (marked by the short arrows in Fig. 4a). In crystals from another $\text{Ba}_5[\text{Si}_8\text{O}_{21}]$ batch, we observed fringes with spacings six and seven times that of a subchain. These can be interpreted as a pair of triple chains or a grouped triple and quadruple chain, respectively, but also as sextuple and septuple chains (Fig. 4c). However, we are not able confidently to distinguish between, for example, a septuple chain and a grouped triple and quadruple chain as the widths are almost the same. Attempts to synthesize ordered Ba silicates with sextuple chains have been unsuccessful. It is thus of interest that occasionally such chains also occur in $\text{Ba}_6[\text{Si}_{10}\text{O}_{26}]$ as errors in the normal quintuple chain structure (Fig. 5).

Note that by imaging of the multiple chains parallel [010] the images consist of projections of several chains which are layered perpendicular to the beam. Thus, in the case of lattice faults, for example, variations in spacing of the fringes correspond not to individual chains, but to layers of chains of differing multiplicity.

Although the Ba chain silicates are ostensibly stoichiometric phases, the occurrence of various widths within a single crystal indicates that compositional variations can and do occur. Such deviations from stoichiometry occur, if the Ba:Si ratio deviates, for example, from $\frac{m+1}{2m} = \frac{5}{8}$ for $\text{Ba}_5[\text{Si}_8\text{O}_{21}]$. The presence of triple chains indicates a ratio $> \frac{5}{8}$, whereas quintuple chains occur if the ratio is $< \frac{5}{8}$. We conclude that some of the synthetic runs were very slightly "off composition" and that these deviations were accommodated coherently by the $\text{Ba}_5[\text{Si}_8\text{O}_{21}]$ crystals. In one case we observed triple, quadruple and quintuple chains within the same crystal, where the triple and quintuple chains are deviations from the normally quadruple chain structure (Fig. 4d); this indicates a local disequilibrium.

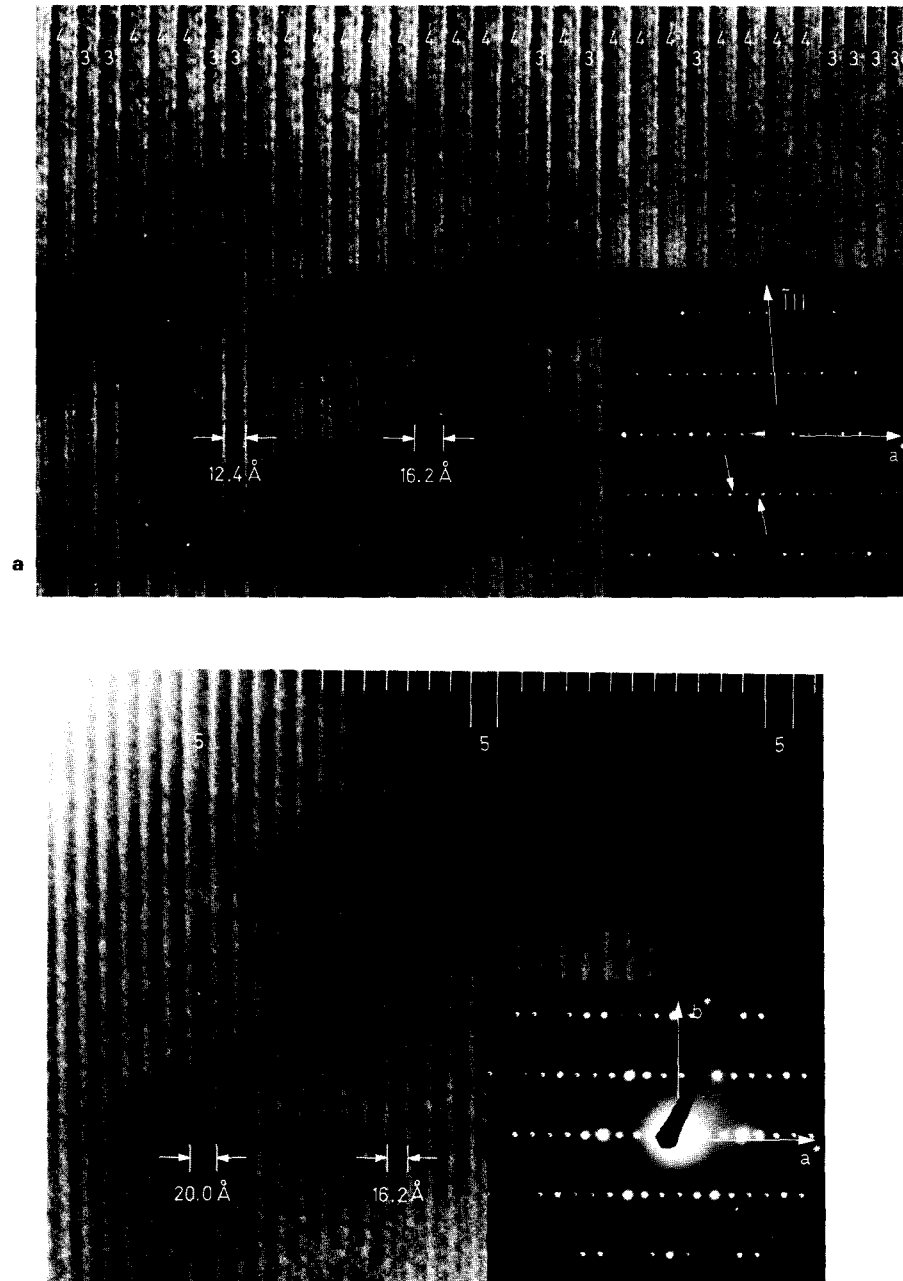
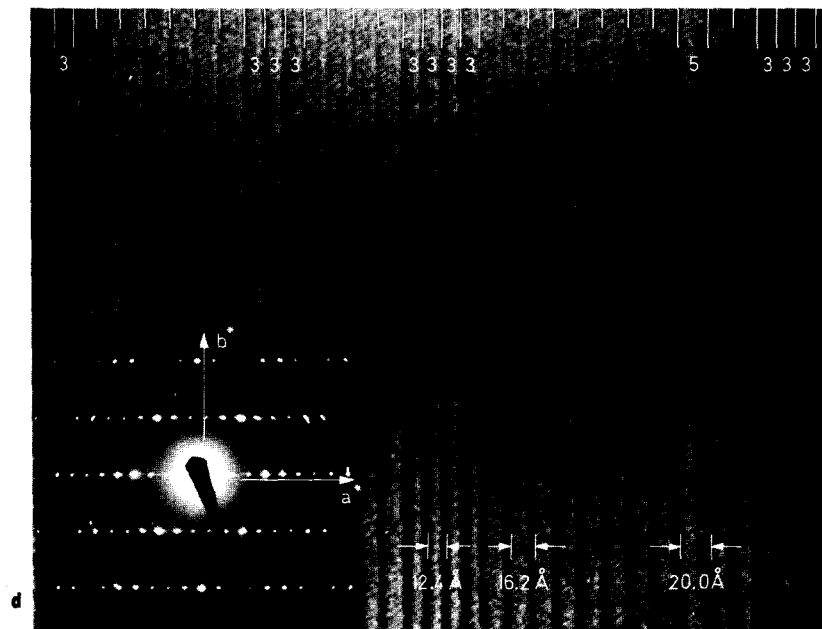
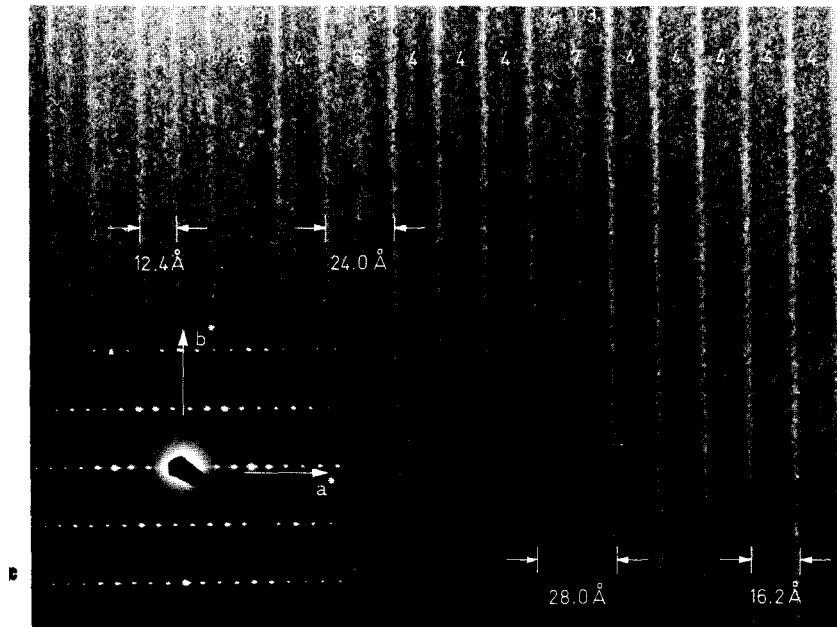


Fig. 4. Lattice faults in the quadruple chain structure of Ba₅[Si₈O₂₁]: a) triple chains; in the diffraction pattern the diffuse reflections marked by the short arrows have the spacings of the triple chain structure. b) isolated quintuple chains. c) Fringes of spacings six and seven (for



explanation see text). d) Coexisting triple and quintuple chains within an area of quadruple chains

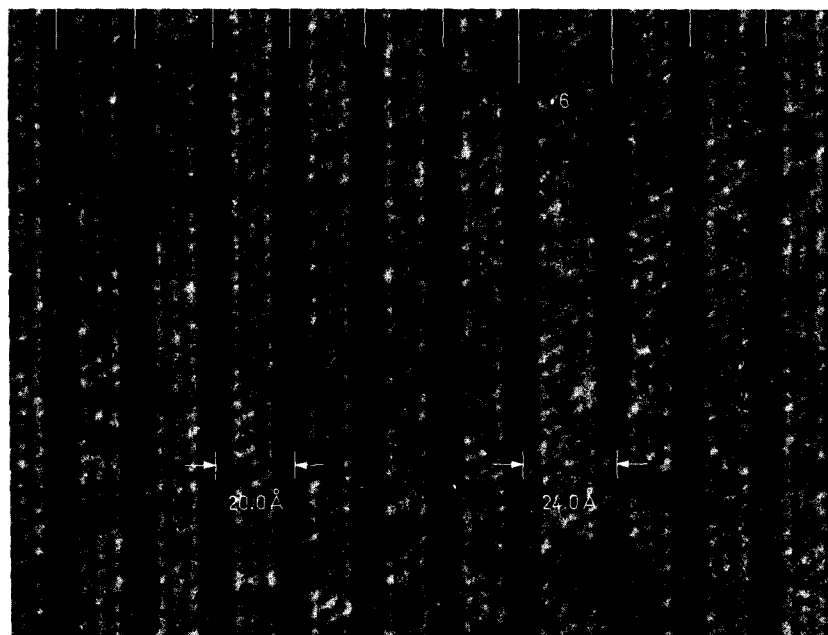


Fig. 5. A lattice fault caused by a layer of sextuple chains in the quintuple chain structure of $\text{Ba}_6[\text{Si}_{10}\text{O}_{26}]$. For diffraction pattern see Figure 3c

Similar slight deviations in stoichiometry have been discussed for the biopyribole minerals (Veblen and Buseck, 1978; Buseck and Veblen, 1978).

Stacking faults

In ordered crystals the packing of the chains along [001] can be described as $\dots A^+ A^- A^+ A^- A^+ A^- A^+ A^- \dots$ (cf. Fig. 1). If an A^- chain is stacked on another A^- , or an A^+ on an A^+ a stacking fault results: e.g. $\dots A^+ A^- A^+ A^- A^- A^+ A^- A^+ A^- \dots$. Such defects are easy to recognize by observing and measuring the spacings of the (001) lattice fringes in *a*-axis images. The distance of the fringes in the c^* direction will then be either $\sim 7 \text{ \AA}$ or $\sim 21 \text{ \AA}$ instead of the $\sim 14 \text{ \AA}$ produced by the normal packing of the chains. Several stacking faults in $\text{Ba}_4[\text{Si}_6\text{O}_{16}]$ are shown in Figure 6.

The good cleavage parallel to (001) of $\text{Ba}_5[\text{Si}_8\text{O}_{21}]$ and $\text{Ba}_6[\text{Si}_{10}\text{O}_{26}]$ made it difficult to have c^* in the diffraction plane and so the degree of stacking disorder remains unknown in these phases.

Conclusions

Results of imaging by high resolution transmission electron microscopy are consistent with the structures of $\text{Ba}_4[\text{Si}_6\text{O}_{16}]$, $\text{Ba}_5[\text{Si}_8\text{O}_{21}]$ and $\text{Ba}_6[\text{Si}_{10}\text{O}_{26}]$

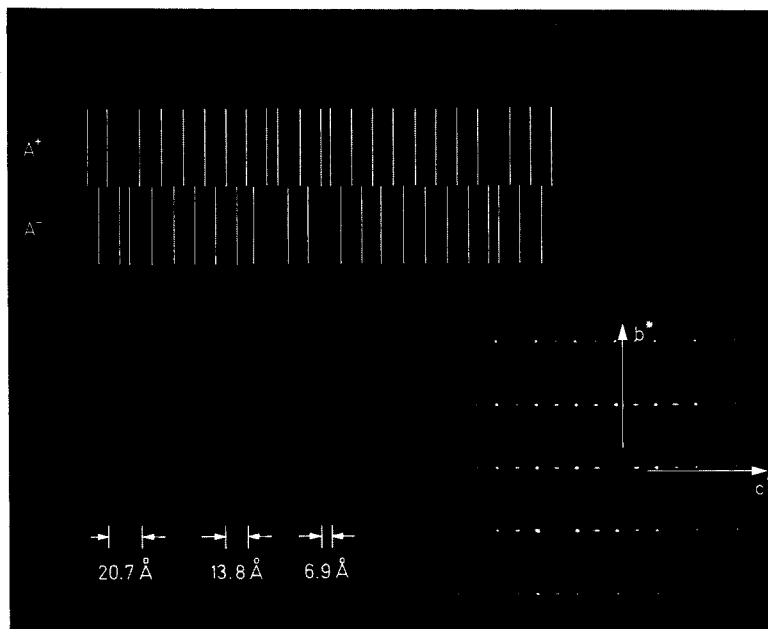


Fig. 6. Stacking faults in $\text{Ba}_4[\text{Si}_6\text{O}_{16}]$. The regions containing stacking errors are resulting from juxtapositioning of either two A^+ or two A^- chains, which are indicated in part of the figure. For further discussion see text

as determined by single crystal X-ray diffraction. The images allow us to confirm that these phases are built up by triple, quadruple and quintuple tetrahedral silicate chains, respectively.

Although large areas of the crystals seem well-ordered, there is also abundant evidence of local disorder. Variations in the stacking order of the A^+ and A^- chains were observed in a -axis images of $\text{Ba}_4[\text{Si}_6\text{O}_{16}]$. Variations in chain multiplicities were observed in c -axis images. In $\text{Ba}_5[\text{Si}_8\text{O}_{21}]$ we observed chains with both higher and lower multiplicities than the normal quadruple chains. In $\text{Ba}_6[\text{Si}_{10}\text{O}_{26}]$, occasional chains wider than the quintuple chains were observed. No deviation from the normal triple chain structure was found in $\text{Ba}_4[\text{Si}_6\text{O}_{16}]$.

Non-stoichiometry occurs in the Ba silicate and is accommodated by incorporation of chains of differing widths in a single crystal. The degree of non-stoichiometry that can occur remains to be determined experimentally. However, the observation of chain width disorder makes it possible to determine that ranges of various compositions can be accommodated within the series $\text{Ba}_{m+1}[\text{Si}_{2m}\text{O}_{5m+1}]$ (cf. introduction to part I, Hesse and Liebau, 1980). Moreover, the occasional occurrence of chains of width six (and perhaps seven) suggests that it may yet be possible to synthesize phases having compositions $\text{Ba}_7[\text{Si}_{12}\text{O}_{31}]$ ($m = 6$) and perhaps $\text{Ba}_8[\text{Si}_{12}\text{O}_{36}]$

($m = 7$). Further crystal chemical aspects of our results are taken into consideration in the general discussion of the crystal chemistry of the Ba silicate compounds in part IV of this series (Liebau, 1980).

A final point is that the images and diffraction patterns described in this paper were obtained from fine-grained powders. They are too fine-grained for single crystal X-ray studies. Thus, using HRTEM it is possible to obtain structural and inferred chemical information from compounds that can not be grown in large crystals. This conclusion has particular applicability to experimental petrology.

Acknowledgements. We thank Dr. R. Roth of the U.S. National Bureau of Standards for sharing his synthetic materials and notes on the Ba silicates. Drs. Liebau and Katscher kindly made their synthetic materials available to us. We thank Drs. F. Liebau and D. Veblen for their helpful comments, both during the project and on the manuscript.

Electron microscopy was performed in the facility in the Center for Solid State Science at Arizona State University, where J. Wheatley was of assistance.

We acknowledge the support of the Deutsche Forschungsgemeinschaft (to M.C.) and grant EAR77-00128 (to P.R.B.) from the Earth Sciences Division of the National Science Foundation.

References

- Buseck, P. R., Iijima, S.: High resolution electron microscopy of silicates. *Am. Mineral.* **59**, 1–29 (1974)
- Buseck, P. R., Veblen, D. R.: Trace elements, crystal defects, and high resolution electron microscopy. *Trace Element Issue, Geochim. Cosmochim. Acta* **42**, 669–678 (1978)
- Drits, V. A., Gonsarov, J. I., Alexandrova, V. A., Chadsi, B. A., Dmitrik, A. L.: A new type of chain silicate. *Kristallographija* **19**, 1186–1193 (1974)
- Hesse, K.-F., Liebau, F.: Crystal chemistry of silica-rich barium silicates. I. Refinement of the crystal structures of $Ba_4[Si_6O_{16}]$, $Ba_5[Si_8O_{21}]$ and $Ba_6[Si_{10}O_{26}]$, silicates with triple, quadruple and quintuple chains. *Z. Kristallogr.* **153**, 3–17 (1980)
- Hutchison, J. L., Irusteta, M. C., Whittaker, E. J. W.: High resolution electron microscopy and diffraction studies of fibrous amphiboles. *Acta Crystallogr.* **A31**, 794–801 (1975)
- Iijima, S., Buseck, P. R.: Experimental study of disordered mica structures by high resolution microscop. *Acta Crystallogr.* **A34**, 709–719 (1978)
- Liebau, F.: Crystal chemistry of silica-rich barium silicates. IV. The influence of condensation degree on the crystal structures of chain and layer silicates of barium. *Z. Kristallogr.* in preparation (1980)
- Veblen, D. R., Buseck, P. R., Burnham, C. W.: Asbestiform chain silicates: new minerals and structural groups. *Science* **198**, 359–365 (1977) plus cover photo
- Veblen, D. R., Burnham, C. W.: New biopyriboles from Chester, Vermont: II. The crystal chemistry of jimthompsonite, clinojimthompsonite, and chesterite, and the amphibole-mica reaction. *Am. Mineral.* 1053–1073 (1978)
- Veblen, D. R., Buseck, P. R.: The multiplicity of pyroxene-amphibole-mica reaction mechanisms. Submitted to 1978 International Mineralogical Association Annual Meeting, Novosibirsk, USSR (1978)